KNOWLEDGE-DRIVEN SEGMENTATION OF THE CENTRAL SULCUS FROM HUMAN BRAIN MR IMAGES

Wei Zuo [1,2] , Qingmao Hu [1] , Aamer Aziz [1] , Kiafock Loe [2] , Wieslaw L Nowinski [1]
Biomedical Imaging Group [1] , Bioinformatics Institute, Singapore
National University of Singapore [2] , Singapore

ABSTRACT: This paper presents a knowledge-driven algorithm to identify and segment the central sulcus (CS) from human brain MR images. The dataset is reformatted along the anterior and posterior commissures (AC-PC) plane first. Then, the 3D region within the two coronal planes passing through the AC and PC is defined as the region of interest (ROI) to search for all the sulci within it. The CS is the sulcus with the largest volume within the ROI. Together with the sulci, grey matter (GM) is included for the region growing in order to deal with the partial volume effect. The GM is removed through skeletonization. Experimental results are given.

Key words: central sulcus; segmentation; MRI; human brain; neuroinformatics.

1. INTRODUCTION

The central sulcus (CS) separates the frontal lobe from the parietal lobe and is an important landmark to consider when localizing brain lesions. Identification and segmentation of the CS is frequently necessary for diagnosis of various pathologic conditions in the brain [1]. Some existing methods recognize the CS by surface arrangement of the sulci [2][6][8].

In this article, we present an automatic algorithm to identify and segment the CS by 3D region growing. The majority of the CS is between the coronal planes passing through the anterior commissure (AC) and posterior commissure (PC) [9] (Fig. 1). 3D brain MR data are reformatted first. Then, the skull and other non-brain tissues are removed. After defining the 3D region of interest (ROI), we segment all the sulci within it by region growing together with gray matter (GM). The CS is taken as the sulcus with the largest 3D volume. Skeletonization is applied for the skeleton of the cerebrospinal fluid (CSF)/GM segmented above. The final result is the union of skeleton and CSF connected to the skeleton.

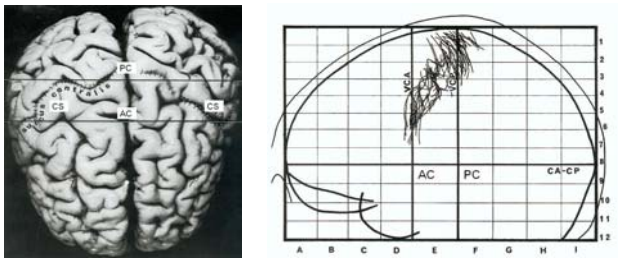

a) b)

Fig. 1 The majority of the CS is between AC and PC: a) top view; (b) statistical location of the CS for 20 cases.

2. METHOD

2.1 Data reformatting

The data are 3D MR volumetric images (Fig. 2a). For each volume, its coordinates of the AC and PC and the midsagittal plane (MSP) are known beforehand.

For the reformatted volume, it will have an isotropic voxel size 1 mm^3 and the following directions of axes: the normal vector of the MSP as the X direction, the line connecting the AC and PC as the Y direction, and the cross product of the X and Y axes as the Z direction.

2.2 Obtaining the mask of brain tissues

The skull is removed in a way similar to that proposed in [7]. Then, 2 thresholds corresponding to the remaining voxels are determined using the Otsu's method [5] to specify the gray level range of white matter (WM), GM and CSF.

The next is to get the mask of the brain tissues which contains the CS. A line parallel to the MSP in an axial slice with a certain distance (5-15 mm) to the MSP will have several intersections with the voxels whose gray levels belong to WM. These intersections are taken as the seeds of WM to perform a 3D region growing of WM. Choose the component with the largest 3D volume as WM. 3D dilation with 5x5x5 structuring elements (SE) is applied on WM followed by opening. The result is the mask of WM with the sulci (the CS included) and GM.

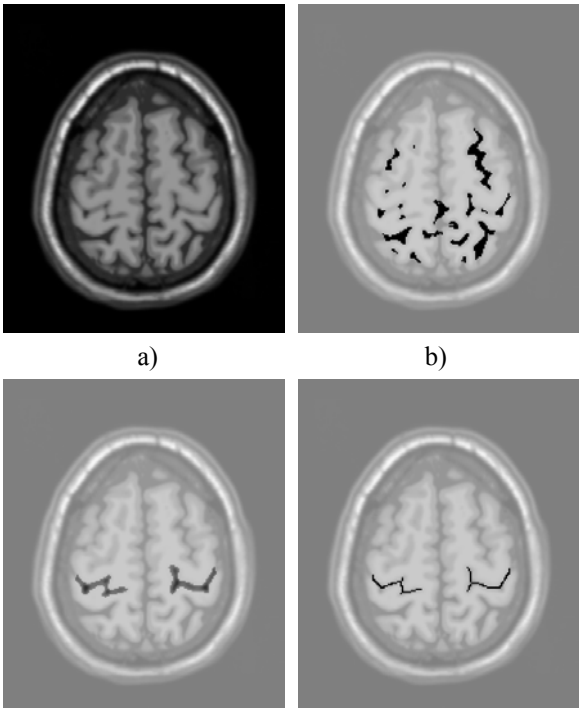

Fig. 2 a) an original axial slice; b) CSF from thresholding; c) the coarse CS grown with CSF and GM; d) skeleton of the coarse CS.

2.3 Segmentation and identification of the CS

As the majority of the CS is between the coronal planes passing the AC and PC, the 3D region between these two coronal planes is defined as the ROI.

2.3.1 Reference slice

Denote $N_{AC\text{-}PC}$ as the slice number of the axial slice passing the AC and PC, $N_{TopTissue}$ the slice number of the top axial slice with brain tissue. Based on our test, the suitable slice number of the axial reference slice (to initiate region growing) can be selected as N, where:

$$N_1=\frac{1}{6}\times N_{AC\text{-}PC}+\frac{5}{6}\times N_{TopTissue}$$

2.3.2 3D look-up table of the boundary voxels

Due to the partial volume effect, sulci may be broken in MR images, so GM is used to aid the segmentation of sulci. We set a 3D look-up table of the boundary voxels of the brain tissue to control the 3D region growing [4].

2.3.3 3D region growing

3D region growing is applied to find all the voxels for each sulcus so that its volume can be obtained.

Assume that $x = X_{MSP}$ is the equation of the MSP. In the reference slice we select 2 lines $x_1=X_{MSP}+20$ and $x_2 =X_{MSP}-20$. There are several intersected voxels with the 2 lines and the sulci within the region between (and near) the AC and PC. Set these intersected voxels as the seeds for the 3D region growing. The criteria for region growing include: 1) the gray level of the voxel must be within the range of the gray level of CSF or GM; 2) the z coordinate of the voxel should not go beyond the range from the z coordinate of the AC to the top axial slice of the brain tissue; 3) the y coordinate of the voxel must be in the range from the y_{AC} to 30 mm posterior to y_{PC} (y_{AC} and y_{PC} are y coordinates of the AC and PC respectively); and 4) the voxel should not go beyond the region defined by the boundary look-up table.

2.3.4 Removal of over-segmentation

Over-segmentation is handled through selection of initial slice and constrained removal described below.

A suitable initial slice is assumed as: there is only a single segment of the CS per hemisphere in this slice and its adjacent slices, and the difference in the area of the CS segmented per hemisphere between this slice and each of its adjacent slices will not exceed a certain value, say, 30%.

Hence, the processing is as follows. Start from the initial slice M: set its adjacent slice N. Calculate the number of the segment(s) of the CS per hemisphere in slice N: if this number is more than one, take the segment in slice N which matches the CS in slice M most and remove the

other segment(s) in slice N. Then calculate the difference in the area of the CS between slice M and N. If the difference is smaller than 30%, there is no over-segmentation in slice N; else dilate the CS in slice M using a 3x3 SE and process "and" operation between this dilated area and the CS in slice N; take the matching part as the CS component in slice N.

Then take N as the reference slice and process its adjacent slice(s) in a similar way.

The CS thus far achieved is called the refined 3D CS.

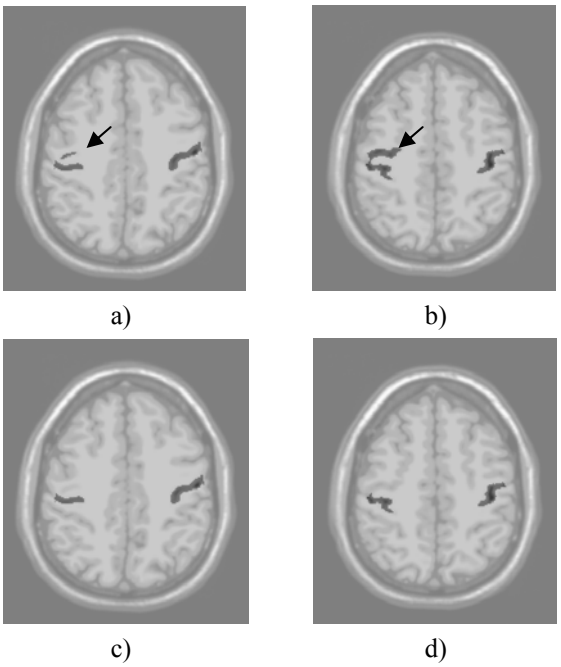

a) b) c) d)

Fig.3 Removal of over-segmentation: a) over-segmentation with multiple segments; b) over-segmentation with a single segment; c) removal of a); and d) removal of b).

2.3.5 2D region growing

2D region growing is applied to get more accurate CS component in each axial slice.

Dilation with a 3x3 SE is applied to the mask of brain tissues in axial slices (2D). The refined CS above is used as the seeds, which is grown within 2D dilated mask with the similar criteria used in previous 3D region growing. After applying the algorithm for over-segmentation removal, the coarse CS is achieved (Fig. 2c).

2. 4 Skeletonization and final CS

Among all the GM in the coarse CS, only some should be kept to connect the CS while the other should be removed. Skeletonization is applied to remove the GM from the coarse CS to get the final CS [3]. The CSF voxels based on thresholding (Fig. 2b) connected to the skeleton are added to the skeleton (Fig. 2d) to yield the final CS.

3. RESULTS

To evaluate our algorithm we use a set of T1-weighted phantom data (http://www.bic.mni.mcgill.ca/brainweb/) with noise (0, 1%, 3%, 5%, 7% and 9%) and inhomogeneity (0, 20% and 40%). The CS could be identified and segmented in 16 out of 18 datasets.

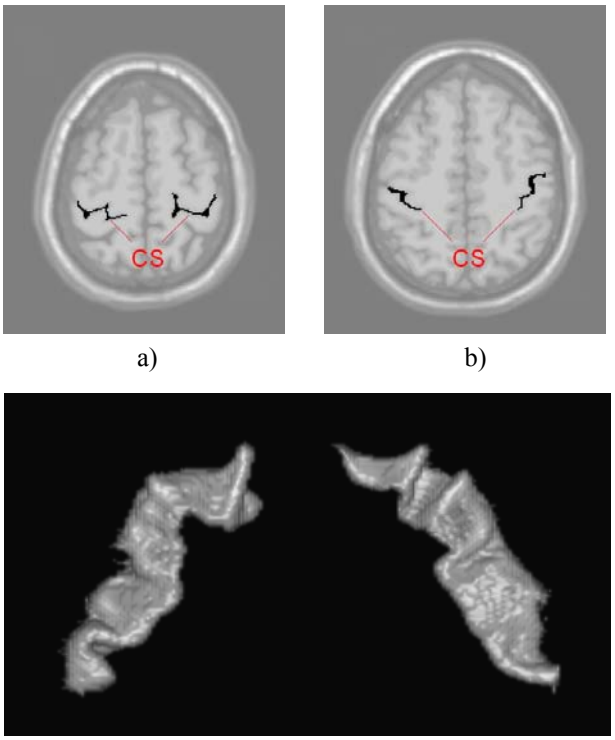

a) b) c)

Fig. 4 The final CS: 2 axial slices with CS overlaid (a, b), and c) the complete CS in 3D.

Figs 4a, b, and c show the final CS in 2 axial slices and the complete CS in 3D, respectively. Compared with manual approaches, the result of our algorithm is visually correct as confirmed by brain anatomy experts.

4. DISCUSSION AND CONCLUSION

It is manifested that the CS has the largest 3D volume within the ROI. Take the dataset with no noise and inhomogeneity for example, the biggest 3D volume of the sulci within the ROI on the left and right hemispheres are 6176 and 5507 mm^3 respectively.

Among the 18 datasets, the CS is successfully identified and segmented from 16 datasets. The 2 failed cases are all with high noise level (9%).

Sensitivity to noise. When the noise level is smaller than 9%, it does not have visible influence on the identification and segmentation. However, when the noise level is 9%, over-segmentation occurs and the algorithm may fail.

Sensitivity to inhomogeneity. The algorithm is quite insensitive to inhomogeneity. It can identify and segment the CS at the inhomogeneity levels 0, 20% and 40% along with additional noise levels 0, 1%, 3%, 5%, and 7%.

Influence of GM. GM is helpful in region growing to connect the broken sulci due to the partial volume effect. Although the GM can cause over-segmentation, its influence can be eliminated through employing the knowledge of possible shapes of CS and skeletonization.

Advantages. This algorithm is fully automatic. As the algorithm is based on the combination of image processing technique and anatomical knowledge, it may well be extended to other imaging sequences and other modalities.

Limitation. This algorithm has not been tested against patient-specific data yet.

To conclude, we have presented a knowledge-driven method for identification and segmentation of the CS from MR images. Comparing the 3D volume proves to be an effective way to identify the CS. Incorporating GM for assisting segmentation of CS proves to be an efficient way to deal with the partial volume effect in brain MR images. Experiments suggest that the algorithm is quite robust to noise and inhomogeneity.

ACKNOWLEDGEMENT

The authors would like to thank Zhenlan Wang for visualization help and Yiping Lu for editorial assistance. We gratefully acknowledge the Biomedical Research Council, the Agency for Science, Technology and Research, Singapore for funding this work.

REFERENCES

[1] Chitoku S, Otsubo H, Sharma RA, Pang E, Rutka JT, Snead OC, "Identification of the Central Sulcus in Adolescents with Epilepsy: MEG Results Confirmed by Cortical Stimulation of Subdural Grid," Proc. 12th International conference on Biomagnetism, pp. 0451-0454, 2000.

[2] Gado M, Hanaway J, Frank R, "Functional Anatomy of the Cerebral Cortex by Computed Tomography," J Computer Assist Tomogr, vol.3, pp. 1-19, 1979.

[3] Hilditch CJ, "Linear Skeletons from Square Cipboards," Machine Intelligence, vol.4, pp. 402-420, 1969.

[4] Hu QM, Langlotz U, Lawrence J, Langlotz F, Nolte LP, "A Fast Impingement Detection Algorithm for Computer-aided Orthopedic Surgery," Computer Aided Surgery, vol. 6, pp. 104-110, 2001.

[5] Otsu N, "A Threshold Selection Method from Gray-level Histograms," IEEE Trans. Syst., Man, Cybern, vol. 9(1), pp. 62-66, 1979.

[6] Ruggiero G, "Encephalography Today," Acta Radiol Suppl, vol.5, pp. 705-715, 1966.

[7] Shan SH, Yue GH, Liu JZ, "Automated Histogram-based Brain Segmentation in T1-weighted Three-dimensional Magnetic Resonance Head Images," NeuroImage, vol.17, pp. 1587-1598, 2002.

[8] Sobel DF, Gallen CC, Schwarts BJ, Waltz TA, Copeland B, Yamada S, Hirschkoff EC, Bloom FE, "Locating the Central Sulcus: Comparison of MR Anatomic and Magnetoencephalographic Functional Methods," AJNR: Am J Neuroradiol, vol.14, pp. 915-925, 1993.

[9] Talairach J, Tournoux P, "Co-planar Stereotaxic Atlas of the Atlas of the Human Brain," Thieme, Stuttgart. New York, 1988.